ELSEVIER

Polymer 43 (2002) 599–607

polymer

www.elsevier.com/locate/polymer

Cohesive properties of Ultem and related molecules from simulations ☆

B.E. Eichinger[a,*], D. Rigby[a], J. Stein[b]

[a]*Accelrys Inc., 9685 Scranton Road, San Diego, CA 92121-3752, USA*
[b]*General Electric-CRD, 1 Research Circle, Niskayuna, NY 12309, USA*

Abstract

The cohesive properties of many engineering plastics are difficult to determine experimentally, as the polymers are frequently insoluble, have high T_gs, and are sometimes poorly characterized. For difficult polymers such as these, molecular modeling can provide useful information of higher quality than might be obtained by other methods. Ultem® is a polyether imide having a very large and relatively stiff repeat unit. We have performed a series of simulations on Ultem and related molecules so as to evaluate the cohesive energy density of the polymer. Small molecular fragments (*N*-phenylphthalimide, 2,2-diphenylpropane, and diphenylether) of the repeat unit were studied to get approximate bounds to be expected for values of the solubility parameter for the polymer. Oligomers up to 4-mers were directly simulated, and the results were used to estimate the properties of the high polymer. These methods yield a value near 22.0 $MPa^{1/2}$ for the solubility parameter of the polymer, lower than has been estimated from group additivity. The interfacial interactions between Ultem and a variety of low molecular liquids have also been evaluated in an effort to identify functional groups that might interact most favorably with the polymer for adhesive applications. These calculations are in good agreement with expectations from solubility parameters. Most significantly, the calculations are fully compatible with experimental observations.

Keywords: Cohesive properties; Ultem; Simulation

1. Introduction

Molecular modeling of bulk materials has advanced to the point where several properties can be reliably computed with an accuracy that rivals experiment [1]. This is especially helpful for those systems that are inherently difficult to study experimentally, and for which experimental data is therefore not available or is of uncertain quality. Foremost amongst difficult systems are the engineering plastics, which are often only soluble in extremely aggressive solvents, have high T_gs, and may be poorly characterized. While these systems are difficult to study experimentally, they also pose challenges to simulations. The structural complexity and rigidity of this class of molecules causes them to relax very slowly, which makes them very difficult to equilibrate in the computer. However, by study of oligomers and related small molecules, with extrapolation to high MW [2], one can partially circumvent many of these problems.

To execute this plan clearly requires a high-quality force field that has been validated for molecules that are structurally homologous to the polymer of interest. We use COMPASS for this purpose, as it has been specifically optimized to provide accurate condensed phase equation of state and cohesive properties for molecules containing a wide range of functional groups [1].

The primary purpose of this research has been to identify potential adhesives or adhesion promoters that might be used with Ultem®. On building a structural model of the surface of the polyether imide polymer, it appeared that the best opportunity for strong physisorption would be provided by H-bond or electrostatic interactions with the imide groups. Structural homology recommended benzyl alcohol as a candidate group that might fulfill these requirements. Furthermore, the published solubility parameters for the polymer [3] (23.7 $MPa^{1/2}$) and benzyl alcohol [4] (24.8 $MPa^{1/2}$) are very similar, suggesting that they should be compatible. To determine whether or not simulations might shed further light on these considerations, we have undertaken a study of the interactions of a range of low molecular liquids with a model for the surface of Ultem. If correct, benzyl alcohol should have the most favorable interactions, while molecules with solubility parameters either higher or lower than benzyl alcohol should be less attracted to the polymer.

☆ This paper was originally submitted to *Computational and Theoretical Polymer Science* and received on 19 October 2000; received in revised form on 13 December 2000; accepted on 15 December 2000. Following the incorporation of *Computational and Theoretical Polymer Science* into *Polymer*, this paper was consequently accepted for publication in *Polymer*.

* Corresponding author. Tel.: +1-858-799-5540; fax: +1-858-799-5100.

0032-3861/02/$ - see front matter
PII: S1089-3156(01)00002-2

The strategy that we chose to adopt for these calculations avoids the direct computation of surface tensions as required by the Dupré equation. This was done to avoid having to calculate the surface tension for the polymer directly, which we considered to be extremely difficult. Instead, we opted to use software to calculate the energy of interaction between the polymer and fluid phases directly, without having to subtract out the polymer–polymer and fluid–fluid contributions. A part of what we will show here is that the method is relatively simple yet very informative.

2. Methods

Simulations were performed with the *Discover* molecular mechanics and dynamics simulation module from Accelrys. Periodic cells containing from about 1500 to 5000 atoms were built with *Amorphous Cell*. The constructs were subsequently refined to provide input for production runs. The smaller cells were used for homogeneous systems and the larger for the heterogeneous (interfacial) systems. The homogeneous systems were built with 3D periodicity, and were equilibrated in the NPT ensemble at 298 K and zero applied pressure using the Berendsen [5] barostat. This equilibration was usually done for 5 ps with dynamics, and this was followed by a data accumulation run lasting at least 100 ps, with configurations being saved every 5 ps. Sun and Rigby [6] have shown that this gives statistically independent energies for systems of small molecules.

Group-based cutoffs were used (the molecules having been subdivided into neutral charge groups), with explicit atom sums being calculated out to 9.5 Å. A 'tail correction' was applied to evaluate the compressive effect on the cell arising from the dispersion interaction between molecules in the cell and all others in the shell from 9.5 Å to infinity. The temperature in all of the simulations was equilibrated with the Andersen algorithm [7], with the velocities being randomized to a Boltzmann distribution every 400–800 fs, depending on the size of the system. The velocity Verlet algorithm [8] was used for integration of the equations of motion. The forces were calculated with the COMPASS forcefield, using parameters given in Appendix A.

Pristine surfaces of organic materials are readily studied with simulations. Methods for constructing polymer surfaces have been described by Mansfield and Theodorou [9] as well as by Mattice and co-workers [10–12]. The method used in the *Amorphous Cell* module of *Materials Studio* [13] is similar to the Mansfield and Theodorou method. A 'glass wall' potential is applied to two plane faces (conventionally taken to be orthogonal to the *c*-axis of the cell) separated by a specified distance of an otherwise periodic box containing the growing polymer. A segment of any molecule that approaches either wall experiences a strong inverse power repulsive force with a singularity outside the box, and this biases the Metropolis ballot criterion encouraging the growing molecule to stay within the box. These slabs or films are then equilibrated to the point where their energy is within the bounds that minimizers can easily handle when the potential is removed or the cells are assembled with other surfaces.

For our studies, 2D boxes of the small molecules were also built using the algorithm described above, whereupon the two slabs were merged and the box extended by 100 Å in the *c*-direction. The fluids were constructed with 1500–2000 atoms each. The glass wall potential between the two interfaces was removed and the surfaces allowed to equilibrate naturally against the vacuum for approximately 2 ps, following which 250-ps production runs were executed. Neutral charge group cutoffs of 9.5 Å were used for propagating the dynamics, with a tail correction being applied to the films in an effort to mimic bulk conditions, as described in more detail below.

This super-cell was treated as a 3D periodic system for the dynamics simulations (overall dimensions ca. 37 Å × 37 Å × 150 Å). The same initial polymer configuration was used for all solvents, and no attempt was made to average over polymer configurations apart from what is realized during the run for any one of the solvents. The thickness of the polymer layer in the equilibrated systems was about 28 Å. The repeat unit is about 21 Å long. If one makes use of the results of Mattice [10–12] on more flexible systems, one concludes that this cell is too thin, relative to the repeat unit length, to have an accurate representation of the configuration statistics of the polymer at the interface. However, to make a good sample of the configuration space of the polymer, or to better represent the surface structure by building a cell with a thickness of several persistence lengths, would have been prohibitively costly. We believe that by using the same initial structure, albeit relatively thin for the polymer, relative differences between the various solvents are meaningful. A representative structure (Ultem plus benzyl alcohol) is shown in Fig. 1.

Simulations on the heterogeneous systems were run in the NVT ensemble at 298 K, with a tail correction applied outside the cutoff of 9.5 Å. This is not an accurate procedure, but was used to ensure that the relatively thin fluid layer would feel an effective pressure equivalent to that in the bulk. Because the system contains a vacuum space, the polymer and solvent are free to expand even though the ensemble is one at constant volume. A pictorial representation of the interactions included and excluded during propagation of the dynamics and evaluation of interaction energies is provided in Fig. 2. During dynamics all interactions, P–P, P–S, and S–S were explicitly evaluated, whereas the interaction energy entailed only the P–S interactions.

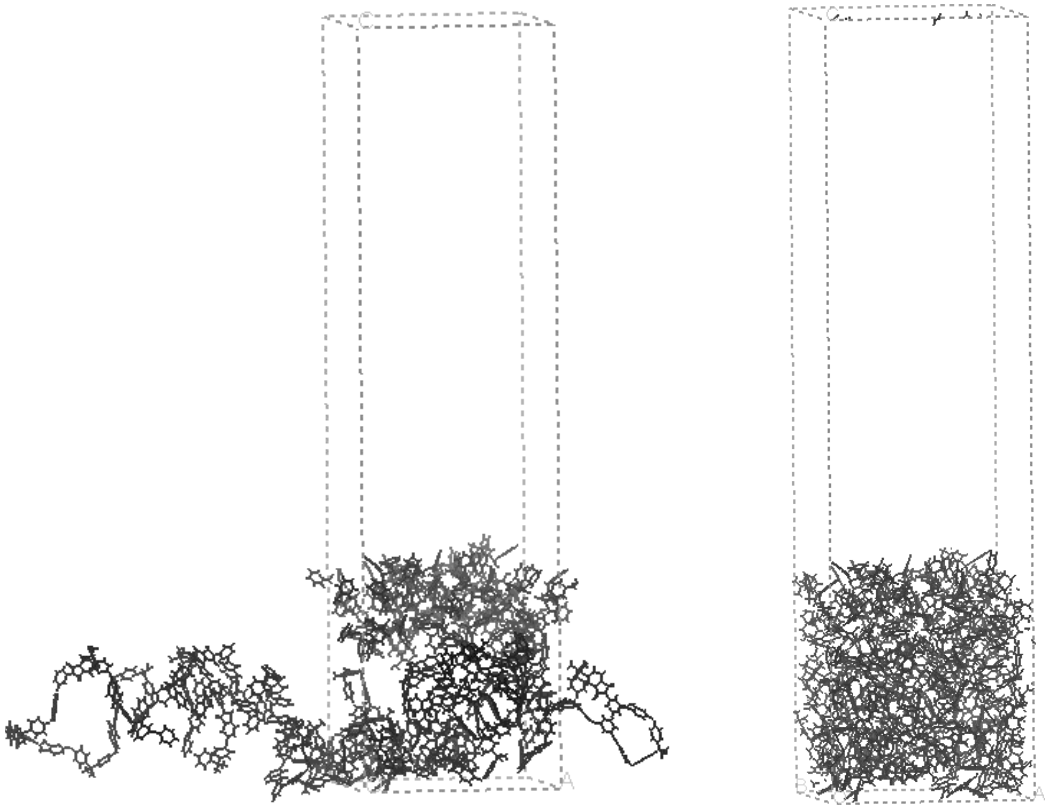

Fig. 1. A representative structure of Ultem interacting with benzyl alcohol. The figure on the left shows the parent molecules superimposed on the cell, while on the right the molecules are packed into the cell with their periodic images.

Every 500 fs the energy of interaction between P (polymer) and S (fluid) layers was evaluated using an 18 Å cutoff without tail correction. Exploration of the dependence of computed interaction energies on this cutoff distance showed that there was no advantage to using a larger cutoff, but a smaller one would have omitted significant contributions to the energy evaluation. This gives a consistent and reasonably accurate measure of the total energy of interaction of the two layers. One run with 225 ethylene glycol molecules gave results essentially identical to that obtained with 150 molecules. A total of 500 energy evaluations were performed for each system (250 ps total simulation time). Visual inspection of the energy as a function of time generally revealed plateaus where the energy fluctuated about a reasonably stationary mean value, and averages over these time intervals were taken. Relatively large excursions of the energy were often seen, and these are associated with diffusion of one or two solvent molecules into the polymer. The polymer film was usually very rough when equilibrated against each of the fluids, and probably had significant voids that allowed diffusion. (This is another aspect of the difficulty in relaxing a bulky molecule below its T_g.) No attempt was made to correct for molecules that had diffused into the polymer matrix; they were included in the calculation of the interactions between polymer and solvent. Since each solvent diffused to some extent, it is probable that the trends in the results are not significantly influenced by this phenomenon.

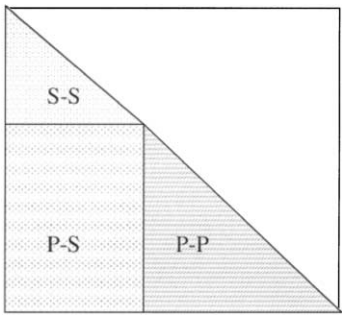

Fig. 2. Pictorial representation of the matrix of intermolecular interactions that was evaluated during the simulation and interfacial energy evaluation. During dynamics, all interactions (P = polymer and S = solvent) were used, as represented by the lower triangular half of the matrix. The interfacial interaction energy was evaluated every 0.50 ps of dynamics from the P–S block of interactions only.

3. Results

The repeat unit [3] of Ultem is shown in structure I. Rather than leave a phenolic group at the chain end, the

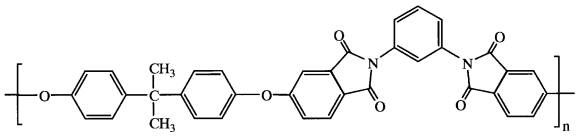

I

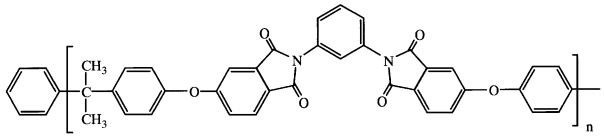

II

oligomers used in calculations were terminated with phenyl groups. That is, oligomers with the structure II were used in the simulations. Neutral charge groups for the phenyl terminated chains were easily assigned.

Owing to the cited difficulties in equilibrating the polymers, it was deemed essential to survey smaller fragments of the repeat unit to establish bounds to be expected for the polymer. To this end, bulk amorphous phases of *N*-phenylphthalimide, 2,2-diphenylpropane, and diphenyl ether were studied. The results are given in Table 1 along with the results for the Ultem oligomers. The solubility parameter for *N*-phenyl-phthalimide, 23.78 $MPa^{1/2}$, provides an upper bound on the solubility parameter for the polymer. This is expected since the less polar units in the backbone will surely cause the solubility parameter to decrease. This contention is verified in Table 1, where it is seen that the 2,2-diphenylpropane unit has a solubility parameter approximately 5 units smaller than the imide moiety. Similarly, the solubility parameter for the diphenyl ether group is smaller by about 2.6 units. A crude estimate for the solubility parameter for the polymer is provided by a weighted average of the values for the two

Table 1
Densities and solubility parameters for Ultem® oligomers and related molecules

Molecule	ρ (g cm^{-3}) Sim.	ρ (g cm^{3}) Lit.	δ ($MPa^{1/2}$) Sim.
N-phenylphthalimide	1.213(0.041)[a]	–	23.78(0.10)
2,2-Diphenylpropane	0.984(0.010)	0.9943[b]	18.82(0.16)
Diphenyl ether	1.093(0.006)	1.075[c]	21.13(0.13)
Ultem 1-mer	1.177(0.013)	–	20.7(0.3)
Ultem 2-mer	1.201(0.006)	–	21.3(0.1)
Ultem 4-mer	1.182(0.008)	1.27[d]	19.0(0.1)

[a] Standard deviations in parentheses.
[b] Ref. [14, p. a-3420]; this value is for the under-cooled liquid.
[c] Ref. [16, p. 1158]; density at 20°C.
[d] Value for Ultem® 1000 from General Electric website: http://www.geplastics.com/products/ultem.html.

imide and ether groups and one diphenylpropane: $\delta \approx [2(23.78 + 21.13) + 18.82]/5 = 21.7$ $MPa^{1/2}$. However, the polymer is denser than the average of these structural units, and an additional correction to increase the solubility parameter by about 10% to account for this effect makes the solubility parameter very near the literature value 23.7 $MPa^{1/2}$. The values computed for the Ultem oligomers can be likewise corrected to the experimental density; this gives values of approximately 21.5 for the 1-mer, 21.9 for the 2-mer, and 19.7 for the 4-mer. The average over the oligomers is about 21.0 $MPa^{1/2}$. We conclude that the best estimate of the solubility parameter for the polymer is about 22.0 $MPa^{1/2}$.

4. Sorption studies

Solubility parameters of the small molecules used in these studies — *iso*-amyl acetate, *n*-amyl acetate, toluene, benzyl alcohol, and ethylene glycol — were evaluated so as to validate the COMPASS force field. The

Table 2
Densities and solubility parameters for solvents and their interactions with Ultem®

Solvent	ρ (g cm^{-3}) Sim.	ρ (g cm^{-3}) Lit.	δ ($MPa^{1/2}$) Sim.	δ ($MPa^{1/2}$) Lit.	$E \times 10^5$ (J cm^{-2})
iso-Amyl acetate	0.856(0.009)	0.8719[a]	16.88(0.20)	16.0[b]	− 2.10(0.03)
n-Amyl acetate	0.865(0.008)	0.8719[a]	17.63(0.22)	17.6[c], 17.1[d]	− 2.23(0.01)
Toluene	0.870(0.008)	0.8622[e]	18.35(0.19)	18.23[f]	− 2.36(0.02)
Benzyl alcohol	1.035(0.008)	1.0416[g]	24.81(0.19)	24.8[b]	− 2.66(0.02)
Ethylene glycol	1.103(0.010)	1.1100[h]	35.00(0.20)	33.89[i], 29.9[j]	− 1.49(0.01)

[a] Ref. [15, p. a-5560].
[b] Ref. [4, p. VII/688].
[c] Ref. [15, p. m-5550].
[d] Ref. [17, p. 135].
[e] Ref. [15, p. a-3290].
[f] Ref. [14, p. m-3290].
[g] Ref. [16, p. 176].
[h] Ref. [15, p. a-5180].
[i] Ref. [15, p. m-5230].
[j] Ref. [17, p. 253].

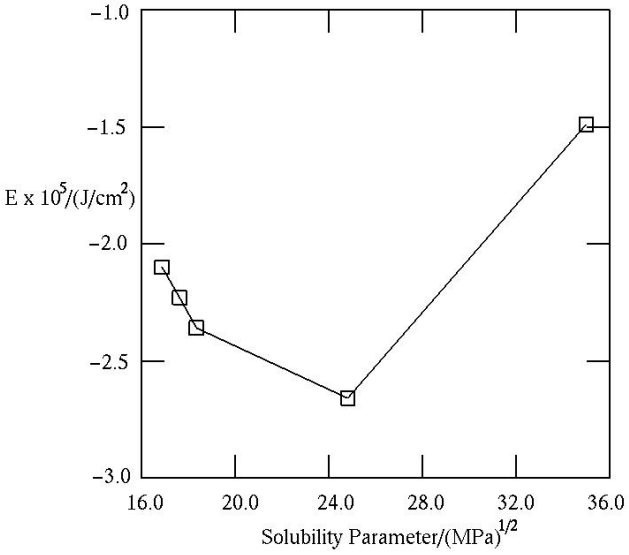

Fig. 3. The energy of interaction between an Ultem® model surface and several low molecular liquids plotted as a function of the solubility parameter. Tabulated results are contained in Table 2.

results of these simulations are shown in Table 2. The table also contains data allowing comparison of densities of the fluids obtained from the NPT simulations with the available literature values. On average, densities agree with the literature to slightly better than 1%, with the largest deviation being for *iso*-amyl acetate. However, there is some doubt as to the reliability of the literature value for this compound, as it is reported to be the same as for the unbranched isomer. Solubility parameters agree with the literature values to within an average of about 1.8%, with the largest deviations (for *iso*-amyl acetate and ethylene glycol) being for fluids having the most uncertain literature values. As previously pointed out by us [2], the experimental values for ethylene glycol are highly scattered. For the other three liquids, solubility parameters from simulations are on average within 0.3% of the reported experimental values.

The interaction energies of the five fluids with the Ultem surface model are contained in the last column of Table 2. A plot of the energies against the solubility parameters of the fluids is shown in Fig. 3. It is seen that the energy appears to have a minimum near $\delta = 24\ \mathrm{MPa}^{1/2}$, i.e. near the value for benzyl alcohol. Qualitative experiments show that benzyl alcohol wets the surface of an Ultem sample, as do the other solvents reported here that have solubility parameters smaller than benzyl alcohol. However, using the same experimental protocols, ethylene glycol is found not to wet Ultem. The simulations are compatible with the experiments.

5. Conclusions

Simulations on Ultem and related compounds suggest that the solubility parameter for the polymer is approximately $22.0\ \mathrm{MPa}^{1/2}$, a value that is slightly lower than that estimated from group additivity methods. Models of interfaces of Ultem in interaction with a variety of low molecular liquids having a range of solubility parameters show that the relatively simple determination of the molecular interaction energies advocated here suffices to identify molecules that interact most favorably with the polymer surface. A good correlation is obtained between the solubility parameters for the liquids and the interface interaction energy, showing that this energy is approximately quadratic in the difference between the solubility parameters for the polymer and the fluids. Simple experiments confirm that all the solvents except ethylene glycol will spread on Ultem. From the range of solvents considered here, simulations suggest that there is a respectably wide window of solubility parameters that are consistent with interfacial compatibility with Ultem. Densities and solubility parameters for a range of low molecular liquids have been obtained from simulations with use of the COMPASS force field, and these are shown to compare very favorably with the literature data.

Acknowledgements

This work was partially supported by SERDP contract No. DAAE3099C0142.

Appendix A

The parameters from the COMPASS force field that have been assigned to the molecules studied here are provided in Tables A1 and A2. Parameters not listed in these tables will be found elsewhere [1,2]. The nomenclature is consistent

Table A1
Definitions of atom types and equivalences

Type	Definition	Equivalences, if any				
		Non-bond	Bond	Angle	Torsion	Out-of-plane
c3′	Carbonyl carbon	c3′	c3′	c3′	c3′	c3′
c3a	Aromatic carbon with three bonds	c3a	c3a	c3a	c3a	c3a

Table A1 (*continued*)

Type	Definition	Equivalences, if any				
		Non-bond	Bond	Angle	Torsion	Out-of-plane
c4	Generic sp3 carbon with four bonds	c4	c4	c4	c4	c4
c43	sp3 carbon with three attached heavy atoms	c43	c4	c4	c4	c4
c44	sp3 carbon with four attached heavy atoms	c44	c4	c4	c4	c4
c4o	sp3 carbon bonded to oxygen	c4o	c4o	c4	c4	c4
h1	Generic hydrogen	h1	h1	h1	h1	h1
h1o	Strongly polar hydrogen bonded to O, F	h1o	h1	h1	h1	h1
n3m	sp3 nitrogen in amides without hydrogen	n3m	n3m	n3m	n3m	n3m
o1=	sp2 oxygen in carbonyl group	o1=	o1=	o1=	o1=	o1=
o2e	Ether oxygen	o2e	o2e	o2	o2	o2
o2h	Hydroxyl oxygen	o2h	o2h	o2	o2	o2
o2s	Ester oxygen	o2s	o2e	o2	o2	o2

Table A2
Parameters (units: bond lengths in Å; angles in grad, except t_0 in degrees; energies in kcal mol^{-1})

Bond dipole increments (in fractions of the charge on the electron)

Atom *i*	Atom *j*	Charge
c3′	o2e	0.112
c3′	c4	0.000
c3′	o1=	0.450
c3′	c3a	0.035
c3′	n3m	0.000
c4o	h1	−0.053
c4o	o2h	0.160
c4o	o2e	0.160
c4o	c4	0.000
c3a	c4o	0.000
c3a	n3m	0.095

Quartic-bond stretch

i	*j*	r_0	k_2	k_3	k_4
c3′	o2e	1.3750	368.7309	−832.4784	1274.0231
c3′	c4	1.5140	312.3719	−465.8290	473.8300
c3′	o1=	1.2160	823.7948	−1878.7939	2303.5310
c3′	c3a	1.4890	339.3574	−655.7236	670.2362
c3′	n3m	1.3850	359.1591	−558.4730	1146.3810
c4o	h1	1.1010	345.0000	−691.8900	844.6000
c4o	o2h	1.4200	400.3954	−835.1951	1313.0142
c4o	o2e	1.4200	400.3954	−835.1951	1313.0142
c4o	c4	1.5300	299.6700	−501.7700	679.8100
c3a	c4o	1.5010	321.9021	−521.8208	572.1628
c3a	n3m	1.3950	344.0452	−652.1208	1022.2242

Quartic angle bend

i	*j*	*k*	t_0	k_2	k_3	k_4
c3′	o2	c4	109.0000	38.9739	−6.2595	−8.1710
c3′	c4	h1	107.8594	38.0833	−17.5074	0.0000
c3′	n3m	c3′	121.9556	76.3105	−26.3166	−17.6944
c3a	c4	o2	109.5000	60.0000	0.0000	0.0000[a]
c3a	c4	h1	111.0000	44.3234	−9.4454	0.0000
c3a	c3a	c4	120.0500	44.7148	−22.7352	0.0000

Table A2 (*continued*)

c3a	o2	c3a	109.5000	60.0000	0.0000	0.0000[a,b]
c3a	c3a	c3′	116.0640	71.2598	−15.8273	2.0506
c3a	c3′	n3m	108.4400	84.8377	−19.9640	2.7405
c3a	c3′	o1=	125.5320	72.3167	−16.0650	2.0818
c3a	c3a	n3m	120.7640	73.2738	−27.4033	13.3920
c3a	n3m	c3′	120.0700	47.1131	−32.5592	13.1257
o1=	c3′	o2	118.9855	98.6813	−22.2485	10.3673
o1=	c3′	c4	119.3000	65.1016	−17.9766	0.0000
o2	c3′	c4	100.3182	88.8631	−3.8323	−7.9802
n3m	c3′	o1=	121.5420	92.5720	−34.4800	−11.1871

Torsion

i	*j*	*k*	*l*	k_1	k_2	k_3
c3′	c3a	c3a	c3′	0.0000	0.0000	0.0000[c]
c3′	c3a	c3a	c3a	0.0000	4.6282	0.0000
c3′	c3a	c3a	h1	0.0000	2.1670	0.0000
c3′	n3m	c3a	c3a	0.0000	0.6500	0.0000
c3′	n3m	c3′	c3a	0.0000	0.0000	0.0000[c]
c3′	n3m	c3′	o1	−0.4066	1.2513	−0.7507
c3′	o2	c4	h1	0.1302	−0.3250	0.1134
c3′	o2	c4	h1	0.9513	0.1155	−0.0000
c3a	c4	o2	h1	0.0000	0.0000	0.0000[c]
c3a	c3a	c4	o2	0.0000	0.3000	0.0000[c]
c3a	c3a	o2	c3a	0.0000	0.5000	0.0000[c]
c3a	c3a	c3′	o1=	0.0000	0.7800	0.0000
c3a	c3a	c3a	n3m	0.0000	3.4040	0.0000
c3a	c3a	c3′	n3m	0.0000	0.0000	0.0000[c]
c3a	n3m	c3′	o1=	0.0000	2.0521	0.0000
c3a	n3m	c3′	c3a	0.0000	0.0000	0.0000[c]
c4	o2	c3′	c4	−2.5594	2.2013	0.0325
c4	o2	c3′	o1=	0.8905	3.2644	0.2646
o1=	c3′	c4	h1	0.0000	0.0000	0.0000
o2	c3′	c4	h1	0.0000	0.0000	0.0000
n3m	c3a	c3a	h1	0.0000	3.4040	0.0000

Out-of-plane

i	*j*	*k*	*l*	k_2	a_0
c3′	c3′	n3m	c3a	0.0000	0.0000
c3′	c3a	c3a	c3a	17.0526	0.0000
c3′	n3m	c3′	c3a	0.0000	0.0000
c3a	c3a	c3a	h1	4.8912	0.0000
c3a	c3a	c4	c3a	7.8153	0.0000
c3a	c3a	h1	c3a	4.8912	0.0000
c3a	c3a	n3m	c3a	17.0526	0.0000
c3a	c3a	c3a	n3m	17.0526	0.0000
c3a	c3′	n3m	o1=	30.0000	0.0000
c3a	c3a	c3′	c3a	17.0526	0.0000
c3a	c3a	o2	c3a	13.0421	0.0000
c3a	c3′	o1=	n3m	30.0000	0.0000
c3a	o1=	c3′	n3m	30.0000	0.0000
c4	c3′	o2	o1=	46.9264	0.0000

Non-bond (9–6)

i	r_0	e_0
c3′	3.9000	0.06400
c3a	3.9150	0.06800
c4	3.8540	0.06200
c43	3.8540	0.04000
c44	3.8540	0.02000
c4o	3.8150	0.06800
h1	2.8780	0.02300
h1o	1.0870	0.00800
n3m	3.7200	0.15000
o1=	3.4300	0.19200

Table A2 (*continued*)

o2e	3.3000	0.12000
o2h	3.5800	0.09600
o2s	3.3000	0.09600

Bond–bond cross-terms

i	*j*	*k*	*ij/jk k*
c3′	o2	c3a	69.5999
c3′	c4	h1	2.2522
c3′	n3m	c3′	25.9530
c3a	c4	o2	0.0000
c3a	c4	h1	2.9168
c3a	c3a	c4	12.0676
c3a	o2	c3a	0.0000
c3′	c3a	c3a	37.8749
c3a	c3′	n3m	0.0000
c3a	c3′	o1=	116.9445
c3a	c3a	n3m	37.8749
c3a	n3m	c3′	0.0000
o1=	c3′	o2	210.1813
c4	c3′	o1=	77.5201
c4	c3′	o2	19.1069
n3m	c3′	o1=	138.4954

Bond–angle cross-terms

i	*j*	*k*	*ij/ijk k*	*jk/ijk k*
c3′	o2	c4	21.5366	−16.6748
c3′	c4	h1	15.5988	14.6287
c3′	n3m	c3′	20.0533	0.0000
c3a	c4	h1	26.4608	11.7717
c3a	c3a	c4	31.0771	47.0579
c3′	c3a	c3a	23.6977	45.8865
c3a	c3a	n3m	35.8865	53.6977
c3a	c3′	o1=	72.8758	76.1093
c3a	c3a	n3m	35.8865	53.6977
o1=	c3′	o2	79.4497	57.0987
c4	c3′	o1=	31.8455	46.6613
c4	c3′	o2	1.3435	4.6978
n3m	c3′	o1=	62.7124	52.4045

Angle–angle cross-terms

i	*j*	*k*	*l*	*ijk/jkl k*
c3a	c3a	o2	c3a	0.0000
h1	c4	c3′	o2	4.7955

End-bond–torsion cross-terms

i	*j*	*k*	*l*	*ij/ijkl*			*kl/ijkl*		
				k_1	k_2	k_3	k_1	k_2	k_3
o1=	c3′	n3m	c3′	−0.7019	0.8305	−0.6874	0.1726	−0.4823	0.2666
h1	c4	o2	c3′	0.9589	0.9190	−0.6015	0.2282	2.2998	−0.4473
c3a	c3a	c4	h1	−0.5835	1.1220	0.3978	1.3997	0.7756	0.0000
c4	c3′	o2	c4	0.1928	1.3187	0.8599	0.0004	−1.0975	0.4831
o1=	c3′	o2	c4	−4.2421	10.1102	1.6824	0.0882	−2.4309	−0.7426
o1=	c3′	c4	h1	0.0536	0.0354	0.3853	2.9036	0.5307	0.1439
o2	c3′	c4	h1	0.4160	−0.1140	0.7099	0.7800	1.3339	0.3268

Middle-bond–torsion cross-terms

i	*j*	*k*	*l*	*jk/ijkl*		
				k_1	k_2	k_3
c3′	c3a	c3a	c3a	0.0000	3.8762	0.0000
o1=	c3′	n3m	c3′	−0.1118	−1.1990	0.6784
c4	c4	o2	c3′	9.9416	2.6421	2.2333
h1	c4	o2	c3′	7.7147	4.2557	−1.0118

Table A2 (*continued*)

c3a	c3a	c4	h1	−5.5679	1.4083	0.3010
o1=	c3′	c3a	c3a	0.0000	2.4002	0.0000
c3a	c3a	c3a	n3m	0.0000	5.2012	0.0000
c4	c3′	o2	c4	1.3445	3.5515	−4.9202
o1=	c3′	o2	c4	0.4552	7.3091	0.2842
o1=	c3′	c4	h1	0.0000	0.0000	−1.0000
o2	c3′	c4	h1	−13.7686	−2.5959	1.1934
h1	c3a	c3a	n3m	0.0000	5.2012	0.0000

Angle–torsion cross-terms

i	*j*	*k*	*l*	*ijk/ijkl*			*jkl/ijkl*		
				k_1	k_2	k_3	k_1	k_2	k_3
o1=	c3′	n3m	c3′	−1.5747	2.3997	−0.2851	−0.3038	−0.0548	−0.3188
c4	c4	o2	c3′	−0.4620	1.4492	−0.6765	−0.0890	−0.9159	0.7229
h1	c4	o2	c3′	−0.4990	2.8061	−0.0401	−0.3142	−0.8699	0.0971
c3a	c3a	c4	h1	0.2251	0.6548	0.1237	4.6266	0.1632	0.0461
c4	c3′	o2	c4	0.9701	−2.5169	1.7195	0.8831	−0.8203	0.2405
o1=	c3′	o2	c4	5.9732	2.7261	1.9052	2.3573	1.0059	−0.0327
o1=	c3′	c4	h1	−2.0667	0.7308	−0.2083	14.4728	0.3339	0.0800
o2	c3′	c4	h1	−0.0241	1.4427	0.1212	13.2959	0.8005	−0.0071

Angle–angle torsion 1

i	*j*	*k*	*l*	*ijk/jkl/ijkl k*
o1=	c3′	n3m	c3′	−3.3556
c4	c4	o2	c3′	−15.7082
h1	c4	o2	c3′	−13.1500
c3a	c3a	c4	h1	−5.8888
c4	c3′	o2	c4	−12.2070
o1=	c3′	o2	c4	−32.9368
o1=	c3′	c4	h1	−23.1923
o2	c3′	c4	h1	−13.9734

[a] These are so-called 'automatic' or generic parameters that have not been explicitly parameterized for the COMPASS force field.

[b] To investigate the sensitivity of computed properties to this bond angle, the optimized geometry of diphenyl ether was obtained with use of DMol[3] with the VWN functional [18], yielding a c3a–o2–c3a angle of 115.5°. The fluid phase of diphenyl ether was re-equilibrated with the angle parameter set to 113° (the difference between this angle and that from the quantum calculation being approximately compensated by non-bond interactions). The changes in density and solubility parameter were negligible.

[c] These are so-called 'automatic' or generic parameters that have not been explicitly parameterized for the COMPASS force field. Since all combinations of quartets of atoms contribute to the total torsional energy for a given bond, the null entries are compensated by contributions from other combinations of atoms.

with the cited references. The paper of Sun [1] describes the function that is used to quantify the potential energy.

References

[1] Sun H. J Phys Chem B 1998;102:7338–64.
[2] Rigby D, Sun H, Eichinger BE. Polym Int 1997;44:311–30.
[3] Bicerano J. Prediction of polymer properties. New York: Marcel Dekker, 1993. p. 157.
[4] Bandrup J, Immergut EH, Grulke EA, editors. Polymer handbook, 4th ed. New York: Wiley, 1999.
[5] Berendsen HJC, Postma JPM, van Gunsteren WF, DiNola A, Haak JR. J Chem Phys 1984;81:3684–90.
[6] Sun H, Rigby D. Spectrochim Acta 1997;A153:1301–23.
[7] Andersen HC. J Chem Phys 1980;72:2384–93.
[8] Verlet L. Phys Rev 1967;159:98–103.
[9] Mansfield KF, Theodorou DN. Macromolecules 1990;23:4430–45.
[10] Zhan Y, Mattice WL. Macromolecules 1994;27:7056–62.
[11] Misra S, Fleming III PD, Mattice WL. J Comput-Aided Mat Des 1994;2:101–12.
[12] Natarajan U, Tanaka G, Mattice WL. J Comput-Aided Mat Des 1997;4:193–205.
[13] Materials Studio is available from Accelrys Inc., San Diego, CA.
[14] Frenkel M, Gadalla NM, Marsh KN, Wilhoit RC, editors. TRC thermochemical tables, hydrocarbons. College Station, TX: Thermodynamics Research Center, 1996.
[15] Frenkel M, Gadalla NM, Marsh KN, Wilhoit RC, editors. TRC thermochemical tables, non-hydrocarbons. College Station, TX: Thermodynamics Research Center, 1996.
[16] The Merck index, 11th ed. Merck & Co., Inc., 1989.
[17] Barton AFM. CRC handbook of solubility parameters and other cohesion parameters. 2nd ed. Boca Raton, FL: CRC Press, 1991.
[18] Delley B. J Chem Phys 1990;92:508–17 (DMol[3] documentation available from Accelrys Inc.).